Propulsion and Power Research 2013;2(2):139–147

http://ppr.buaa.edu.cn/

Propulsion and Power Research

www.sciencedirect.com

ORIGINAL ARTICLE

# Development of high intensity low emission combustor for achieving flameless combustion of liquid fuels

V. Mahendra Reddy, Sudarshan Kumar*

*Department of Aerospace Engineering, Indian Institute of Technology, Bombay, Powai Mumbai – 400076, India*

Received 9 January 2013; accepted 1 April 2013
Available online 5 June 2013

**KEYWORDS**

Swirl flow combustion;
Flameless combustion;
Internal recirculation;
Liquid fuels;
Spray combustion;
Low emissions

**Abstract** This paper presents the experimental and numerical results for a two stage combustor capable of achieving flameless combustion with liquid fuels for different thermal heat inputs of 20, 30, 40 and 60 kW and heat release density of 5–15 MW/m$^3$. Combustion characteristics and pollutant emissions are studied for three different fuels, kerosene, diesel and gasoline. The influence of droplet diameter on pollutant emissions at all conditions is studied. The fuel and oxidizer are supplied at ambient conditions. The concept of high swirl flows has been adopted to achieve high internal recirculation rates, residence time and increased dilution of the fresh reactants in the primary combustion zone, resulting in flameless combustion mode. Air is injected through four tangential injection ports located near the bottom of the combustor and liquid fuel is injected through a centrally mounted pressure swirl injector. Computational analysis of the flow features shows that decrease in the exit port diameter of the primary chamber increases the recirculation rate of combustion products and helps in achieving the flameless combustion mode. Based on preliminary computational studies, a 30 mm primary chamber exit port diameter is chosen for experimental studies. Detailed experimental investigations show that flameless combustion mode was achieved with evenly distributed combustion reaction zone and uniform temperature distribution in the combustor. Pollutant

*Corresponding author: Tel.: +91 22 25767124.
E-mail address: sudar@aero.iitb.ac.in (Sudarshan Kumar).

Peer review under responsibility of National Laboratory for Aeronautics and Astronautics, China.

Production and hosting by Elsevier


http://dx.doi.org/10.1016/j.jppr.2013.04.006

emissions of CO, $NO_x$, $C_xH_y$ are measured and compared for all operating conditions of different fuels and different thermal inputs. The acoustic emission levels are reduced by 6–8 dB as combustion mode shifts from conventional mode to flameless combustion mode.


## 1. Introduction

Flameless combustion is a novel combustion mode, with evenly distributed combustion reaction zone results uniform temperature distribution. Flameless combustion is achieved through increased internal recirculation of hot combustion products resulting in the dilution and preheating of fresh reactants. This helps in suppressing the formation of $NO_x$ through thermal route and CO emissions [1–12]. The reaction zone is almost invisible and uniformly distributed throughout the volume of the combustor [13–16]. To achieve flameless combustion mode, the combustion products need to be recirculated in large quantities to ensure that the flame is blown-off from primary combustion zone [1–3,5,16,17]. This reduces the concentration of the reactants to such an extent that combustion is not initiated until mixing process is complete and thereby reducing the reaction rate. Combustion reaction proceeds only when the local temperature is above the auto ignition temperature of the fuel [7]. This helps in avoiding the formation of sharp high temperature zones in the combustion chamber.

Flameless combustion with gaseous fuel has proven that irrespective of fuel quality sustained flameless combustion mode can be achieved in the combustor [7,9,14]. Preheating and dilution of the fuel and oxidizer is an important parameter to achieve the flameless combustion mode. This process is strongly influenced by internal recirculation of combustion products and mixing in the combustor. The mixing process in flameless combustion with gaseous fuel is relatively easy, because both fuel and oxidizer are in the same gaseous phase. Combustion of liquid fuels depends on fuel properties like, surface tension, viscosity, boiling point. The Sauter mean diameter (SMD) of the droplets in a spray is a function of fuel properties [18]. The properties of various liquid fuels considered for present experimental studies are summarized in Table 1. At an injection pressure of $P_{inj}=9$ bar (900 kPa), SMD of gasoline spray is 14 μm. The SMD of kerosene and diesel sprays is 20 and 26 μm respectively at the same injection pressure. Evaporation rate of droplets is a function of boiling point and surface area to volume ratio ($A_s/V$) of the droplet size. $A_s/V$ of the gasoline droplets is $4.2 \times 10^5$, whereas for kerosene and diesel droplets, the value of this parameter is $3 \times 10^5$ and $2.3 \times 10^5$ respectively. The evaporation time of these droplets increases with boiling point temperature and SMD of the droplet [19]. Spray cone angle also plays an important role in the entrainment and droplet evaporation rate.

Achieving flameless combustion with liquid fuels involves many complex processes such as fuel injection, droplets distribution, droplet evaporation, mixture formation and subsequent combustion with preheating and dilution of reactants. In case of conventional combustion, flame stabilizes in a narrow zone near the fuel nozzle resulting in the formation of a high temperature zone neat the nozzle exit. Due to this, fuel droplets evaporate quickly in conventional combustion mode and get combusted near the nozzle exit [7]. However, in case of recirculation of hot combustion products, reaction zone is distributed throughout the volume of the chamber [1,2,20]. The peak flame temperature and its fluctuations are relatively lower as compared to conventional combustion mode [1,2,6,9]. The droplet evaporation rate is expected to be lower in this mode as compared with conventional combustion mode due to lower peak temperature. Therefore, to sustain the flameless combustion mode with liquid fuel, large residence time is required as compared with gaseous fuel case.

Although substantial amount of work on flameless/moderate or intense low-oxygen dilution (MILD) combustion with gaseous fuels has been reported in the literature [1–12], very little work with liquid fuels is available in the literature [13,14]. Since most of combustion systems operate with liquid fuels, it is important to develop flameless

**Table 1** Characteristics of various fuels.

| Property | Kerosene | Diesel | Gasoline |
|---|---|---|---|
| Density/(kg/m$^3$) | 800 | 860 | 803 |
| Kinematic viscosity/(m$^2$/s) | $2.71 \times 10^{-6}$ | $3.64 \times 10^{-6}$ | $0.8 \times 10^{-6}$ |
| Surface tension/(mN/m) | 25 | 23 | 21 |
| Flash point/K | 334 | 398 | – |
| Boiling point/K | 433 | 558 | 364 |
| SMD/μm ($P_{inj}=9$ bar) | 20 | 26 | 14 |
| Ratio of surface area to volume/m$^{-1}$ ($A_s/V$) | $3.0 \times 10^5$ | $2.3 \times 10^5$ | $4.2 \times 10^5$ |
| Evaporation time/ms $\tau_{evap}$ at $T_\infty=1000$ K | 8.1 | 11.6 | 5.3 |

combustion systems with liquid fuels. Recent investigations on flameless combustion with liquid fuels have been reported in the literature [14–16]. However, the influence of liquid fuel properties, droplet diameter and spray cone angle on flameless combustion has not been adequately discussed in the literature.

In the present study, a combustion system operating in flameless combustion mode with different liquid fuels is developed with heat release intensity of 5–15 MW/m$^3$ and air supplied at ambient temperature. A two stage swirl flow combustor configuration developed in our previous study (Reddy et al. [16]) is considered in this study and shown in Figure 1. Swirl flow pattern provides large residence time and better mixing [16,21–23]. In the present work, the combustor is tested for four different thermal inputs of 20, 30, 40 and 60 kW. Sustainability of flameless combustion with three different fuels of kerosene, diesel and gasoline is observed for all thermal input conditions. Computational analysis is carried out to understand the flow features of the reacting flow and the variation of reactants dilution ratio with its effect on flameless combustion mode. The main objective of this study is to understand the influence of fuel properties and droplet diameter on emissions from combustor is analyzed for all operating conditions. CO, $NO_x$ and $C_xH_y$ emissions are measured and analyzed.

## 2. Reactants dilution ratio ($R_{dil}$)

Internal recirculation of combustion products plays a key role in achieving flameless combustion mode. Therefore, reacting flow computational studies have been carried out to understand the flow features inside these combustors with an aim to optimize the reactant dilution ratio. A general purpose CFD code Fluent-6.3 is used for solving three-dimensional (3D) Navier-Stokes equations along with energy and species conservation equations in a finite-volume domain. Tetrahedral mesh is used for meshing of the 3D computational fluid domain. A number of computations were carried out using tetra mesh with a mesh size of 1.2 mm and the mesh is refined after every simulation. The number of cells for computations was varied from 2 to 4.5 million elements. All results with approximately 3.5 million grid points were independent of the grid used. Since the main focus of this computational analysis is to study the flow pattern in the combustor, only kerosene ($C_{12}H_{23}$) is considered as fuel for all thermal input conditions and equivalence ratio variations. Constant mass flow inlet condition with mass flow rate normal to the boundary surface is applied at the tangential air inlets. A pressure outlet based boundary condition is applied at the exhaust port. The oxidizer is assumed to be air at a total pressure of 101325 Pa. The oxidizer (air) enters the combustor at different temperatures for different operating conditions. No slip wall boundary condition is applied at all walls and a constant temperature boundary condition is applied. The solution is considered to be converged when RMS residuals of the flow, species and energy balance of the system are of the order of $10^{-5}$ and $10^{-6}$, respectively, and there are no appreciable changes in the respective residuals. A non-premixed droplet evaporation and combustion following spherical-law is considered along with a probability density function based model. Ignition is simulated by creating a high temperature patch in the fluid domain near the fuel injection port. For simplicity, a constant droplet diameter is assumed with droplet diameter of 20 μm. Fuel injection is simulated to be of solid cone type spray with a cone angle of 45°.

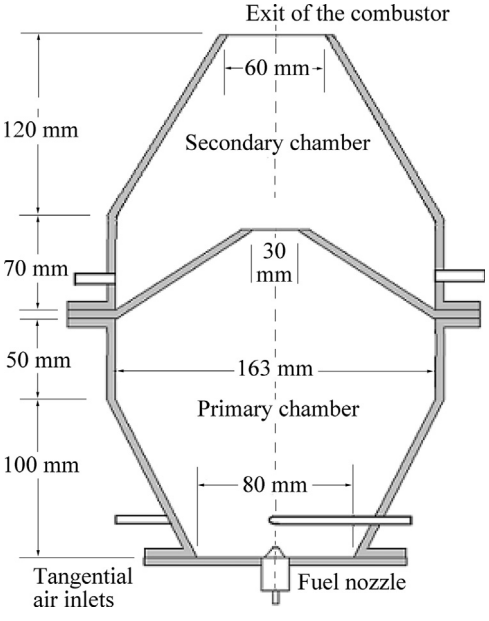


**Figure 1** Schematic diagram of two stage combustor [16].

Reactant dilution ratio ($R_{dil}$) is the ratio of net mass flow rate interaction in a plane to the total mass flow rate of the reactants. It is a measure of the recirculation of the combustion products and their interaction with the fresh mixture [2,16]. Reactant dilution ratio is calculated as follows.

$$R_{dil} = \frac{\dot{m}_{axial} - (\dot{m}_{ox} + \dot{m}_f)}{(\dot{m}_{ox} + \dot{m}_f)} \quad (1)$$

$$\dot{m}_{axial} = \iint \rho v_{axial} dy dz \quad (2)$$

Here $\dot{m}_{axial}$ is total mass flow interacting at a given plane, $\dot{m}_{ox}$ and $\dot{m}_f$ are the mass flow rates of oxidizer and fuel respectively. $\rho$ and $V_{axial}$ are the density and axial velocity.

### 2.1. Influence of exit port diameter of primary chamber

A swirl based two-stage combustor configuration is considered in this study (Figure 1). Based on the outlet diameter of primary chamber, three different combustor configurations are considered, D30, D45 and D60. Computational studies of previous study show that D30 combustor is an optimal configuration to achieve flameless combustion with liquid fuel. The variation of reactants dilution ratio for

D30, D45 and D60 combustors are shown in Figure 2. Reactants dilution ratio, $R_{dil}$ and length of recirculation zone increases with a decrease in the exit port diameter of the primary chamber because reduction in exit port size increases the reverse flow within the combustor. A maximum dilution ratio of 1.89 is achieved for D60 case at an axial location of 50 mm and it reduces sharply to 0.42 at an axial length of 110 mm. For D30 case, a maximum dilution ratio of 2.25 is achieved at an axial position of 70 mm. $R_{dil}$ is greater than 2.0 for a zone length of 30 mm as seen in Figure 2. $R_{dil}$ is greater than 1.0 for a zone length of 100, 80 and 70 mm respectively for D30, D45 and D60 combustors.

### 2.2. *Influence of thermal input and equivalence ratio*

The diameter of tangential air inlet is maintained constant for all operating conditions (5 mm). The inlet air mass flow rate and inlet velocity increases for high thermal heat input and lean equivalence ratio at a thermal heat input. An increase in the inlet velocity increases the swirl intensity resulting in increased recirculation zone. The vertex breakdown zone moves towards the bottom of the combustor. The variation of the reactant dilution ratio with global equivalence ratio is shown in Figure 3. For lean equivalence ratios with fixed thermal input, the reaction intensity (heat release intensity) remains constant and the local turbulence increases due to increased oxidizer flow rate. Therefore, the reactant dilution ratio increases for leaner mixtures. For case of 20 kW thermal input, 2.25, 2.61, 2.72, 2.95 of reactants dilution ratios are observed for equivalence ratios of 0.98, 0.81, 0.73 and 0.66 respectively, at an axial position of 0.07 m, shown in Figure 3. The reactants dilution ratio, $R_{dil}$ and length of high recirculation zone decreases with an increase in the thermal input as shown in Figure 4. The intensity of combustion reaction increases with an increase in the thermal input (constant volume of the combustor). Therefore the reactants dilution ratio reduces with an increase in the thermal input. At an axial position of 0.07 m, $R_{dil}$ for 20, 30 and 40 kW are 2.25, 1.97 and 1.86 respectively, shown in Figure 4. A brief summary of length of recirculation zone for different operating conditions is given in Table 2.

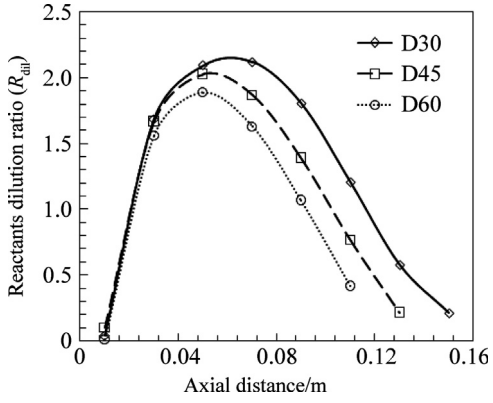


**Figure 2** Variation of reactants dilution ratio ($R_{dil}$) along the combustor axis for various combustors (D30, D45 and D60) [16].

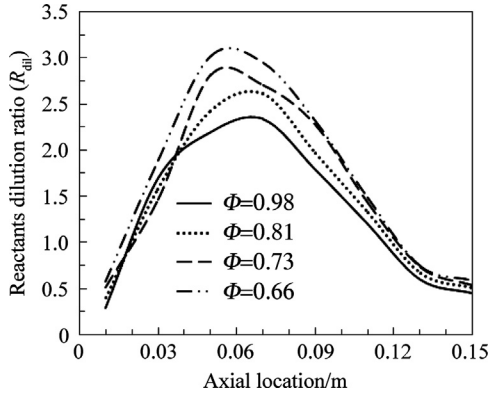


**Figure 3** Variation of reactants dilution ratio ($R_{dil}$) for various equivalence ratios at 20 kW thermal input.

## 3. Experimental setup details

A schematic diagram of the experimental setup is shown in Figure 5. The combustor is placed vertically on a test stand as shown in the Figure 5. Mass flow rate of air controlled with electronic mass flow controller operated by a command module through a personal computer. Liquid fuel is stored in a pressurized steel tank. The fuel flow is

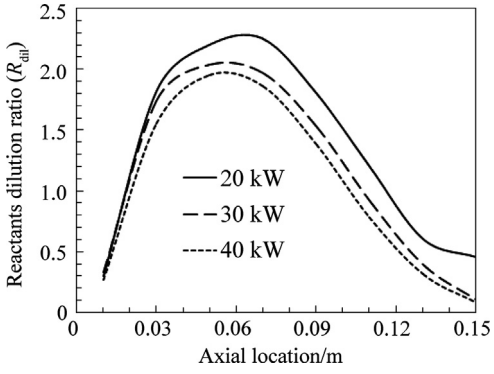


**Figure 4** Variation of reactants dilution ratio ($R_{dil}$) for different thermal inputs ($\Phi$=0.98).

**Table 2** Comparison of length of recirculation zone for different combustors and different operating conditions.

| Combustor configuration | $Q_{th}$/kW | $\Phi$ | $R_{dil}$> 1 mm | $R_{dil}$> 1.5 mm | $R_{dil}$> 2 mm | $R_{dil}$> 2.5 mm | $R_{dil}$> 3 mm |
|---|---|---|---|---|---|---|---|
| D60 | 20 | 0.98 | 72 | 40 | Nil | Nil | Nil |
| D45 | 20 | 0.98 | 81 | 60 | 14 | Nil | Nil |
| D30 | 20 | 0.98 | 96 | 78 | 36 | Nil | Nil |
| D30 | 30 | 0.98 | 89 | 63 | 35 | Nil | Nil |
| D30 | 40 | 0.98 | 81 | 56 | Nil | Nil | Nil |
| D30 | 20 | 0.81 | 102 | 78 | 50 | 24 | Nil |
| D30 | 20 | 0.73 | 100 | 81 | 61 | 38 | Nil |
| D30 | 20 | 0.66 | 108 | 87 | 70 | 55 | 18 |

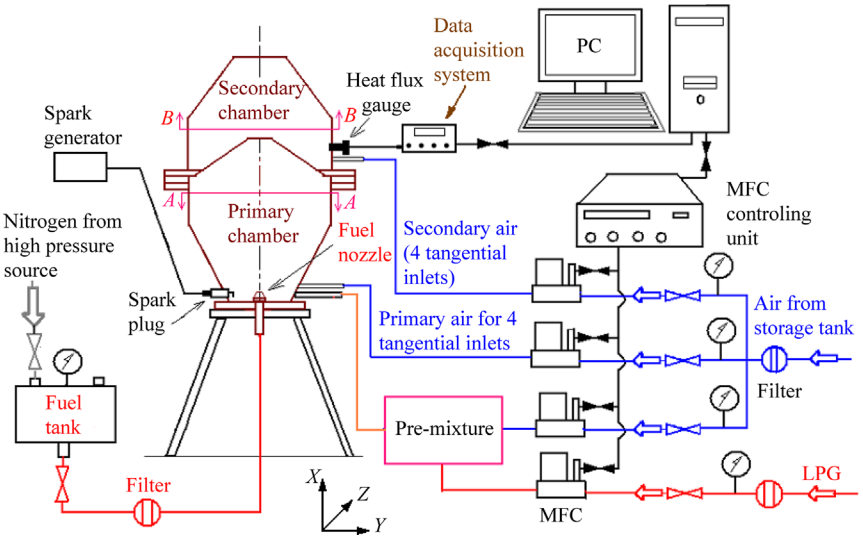


**Figure 5** Schematic diagram of experimental setup.

controlled through a ball valve during the combustor operation. The combustor is tested for four different heat release densities of 5, 7.5, 10 and 15 MW/m$^3$ and with three different liquid fuels of kerosene, diesel and gasoline. Pressure swirl injectors with a mass flow rate of 1.72, 2.72, 3.54 and 5. 23 kg/h at 9 bar injection pressure are used to inject the fuel in the combustor. Fuel injector is mounted centrally at the bottom of the combustor. The spray cone angle of the injector is 45° and the SMD at 9 bar pressure is in the range of 14–26 μm (measured with Malvern Mastersizer). The air is drawn from high pressure storage tank and controlled through electric mass-flow controllers. The combustor is initially ignited with spark-plug and run with premixed LPG-air mixture. To ensure initial flame stabilization, stoichiometric (1:15.61 ratio of fuel and air by mass) flow rates of liquid fuel and air are maintained. Exhaust gas composition is measured with Quintox KM-9106 gas analyzer with an $O_2$ analyzer (0%–25% range, 0.1% accuracy), CO analyzer (0–10000 ppm range, accuracy ±5% of reading), NO analyzer (0–5000 ppm, ±5 ppm accuracy), a $C_xH_y$ analyzer (0–50,000 ppm), and a $CO_2$ analyzer. Continuous online measurement of the sample gas has been carried out. Temperature measurements are carried out with R-type (diameter = 1 mm) thermocouple. The measured temperature is corrected for convection and radiation losses from the thermocouple junction. Acoustic emissions are measured with a fast response sound level instrument (Lutron, SL-4001, $\tau_{response} = 200$ ms) for different combustion modes. The sound level meter is placed 100 mm away from the exit plane of the combustor.

## 4. Experimental observations

Experiments are conducted for all operating conditions with a total fuel consumption of 760 mL for a duration of 21 minutes. Tangential velocity of air inlets has been fixed in the range of 50–90 m/s. The heat from the intermediate cone (middle plate) is helpful in improving the evaporation of liquid fuel droplets in the primary chamber as a part of the spray directly strikes with it. Secondary air is injected near the intermediate cone. The combined effect of secondary air injection and fuel spray helps in maintaining the temperature of middle cone within the permissible limits. The reactant dilution ratios are relatively smaller for D45 and D60 cases as compared to D30 case. Therefore, for D60 case, a thick yellowish diffusion flame is observed along the central axis of the combustor and it is extended till the exit of the secondary chamber. Similarly, various experiments on D45 case showed that it was not possible to achieve flameless combustion mode. However, the size of yellowish diffusion flame was reduced significantly and it became a wick-type diffusion flame at the center of the combustor. $R_{dil}$ increases with a decrease in the exit port diameter of the primary chamber. The increased preheating and dilution of the fuel and oxidizer due to high $R_{dil}$ improves the droplet evaporation rate and spreads the reaction zone uniformly throughout the combustor volume. Therefore, the conventional yellow flame gradually disappears and it transforms into flameless combustion mode. Due to this, flameless combustion mode is achieved for D30 case. The photographs of flame transition from conventional to flameless mode for D30 case is shown in Reddy et al. [16]. The fuel injection nozzle on the bottom injection plane of the combustor was clearly visible and reaction zone is completely transparent in the combustor.

## 5. Results and discussion

### 5.1. Emission measurement

The variation of the composition of various combustion species such as CO, $NO_x$ and $C_xH_y$ (UHC) at the exit of the combustor for different thermal heat inputs along with different equivalence ratios is shown in Figure 6. Emissions

for different fuels kerosene, diesel and gasoline are compared. Pollutants emission from the combustor is studied for different thermal inputs of 20, 30, 40 and 60 kW. Reactant dilution ratio is a key parameter to achieve the flameless combustion mode. An increase in the thermal input results in a decrease in the reactant dilution ratio, $R_{dil}$ and residence time. Therefore, CO and $NO_x$ emissions are observed to increase with an increase in the thermal input. Sauter mean diameter (SMD) of kerosene, diesel and gasoline are 21, 27 and 14 μm respectively. The droplet evaporation rate is a function of surface area to volume ratio of droplet and boiling point temperature of fuel. Since the diameter and boiling point of diesel droplets is larger, higher emissions are observed for diesel combustion as compared with kerosene and gasoline fuels. At a particular thermal input, the flame temperature decreases with a decrease in the global mixture equivalence ratio (shown in Figure 7), hence lower $NO_x$ emissions are observed for leaner mixtures. For leaner mixtures, mixture residence time decreases and reactant dilution ratio ($R_{dil}$) increases with an increase in the mass flow rate of oxidizer. Both high temperature and large residence time are required for complete combustion in highly diluted environments. The combined effect of these parameters leads to a slight increase in CO emissions as seen in Figure 6 for the range of equivalence ratios investigated in the present work. The flame sustainability is observed for three types of fuels with different thermal inputs of 20, 30, 40 and 60 kW. The combustion sustained in the chamber for thermal inputs of 40, 30, 60 kW respectively for kerosene, diesel and gasoline. The droplet diameter and boiling point of gasoline is relatively smaller as compared with diesel and kerosene fuels. Hence, quick evaporation and mixing results in stabilized flameless combustion mode even for high thermal inputs (60 kW) and low equivalence ratios of 0.6. On the contrary, the droplet diameter and boiling point of diesel is high, therefore, the flameless combustion mode is sustained up to 30 kW thermal input. For kerosene and diesel fuels,

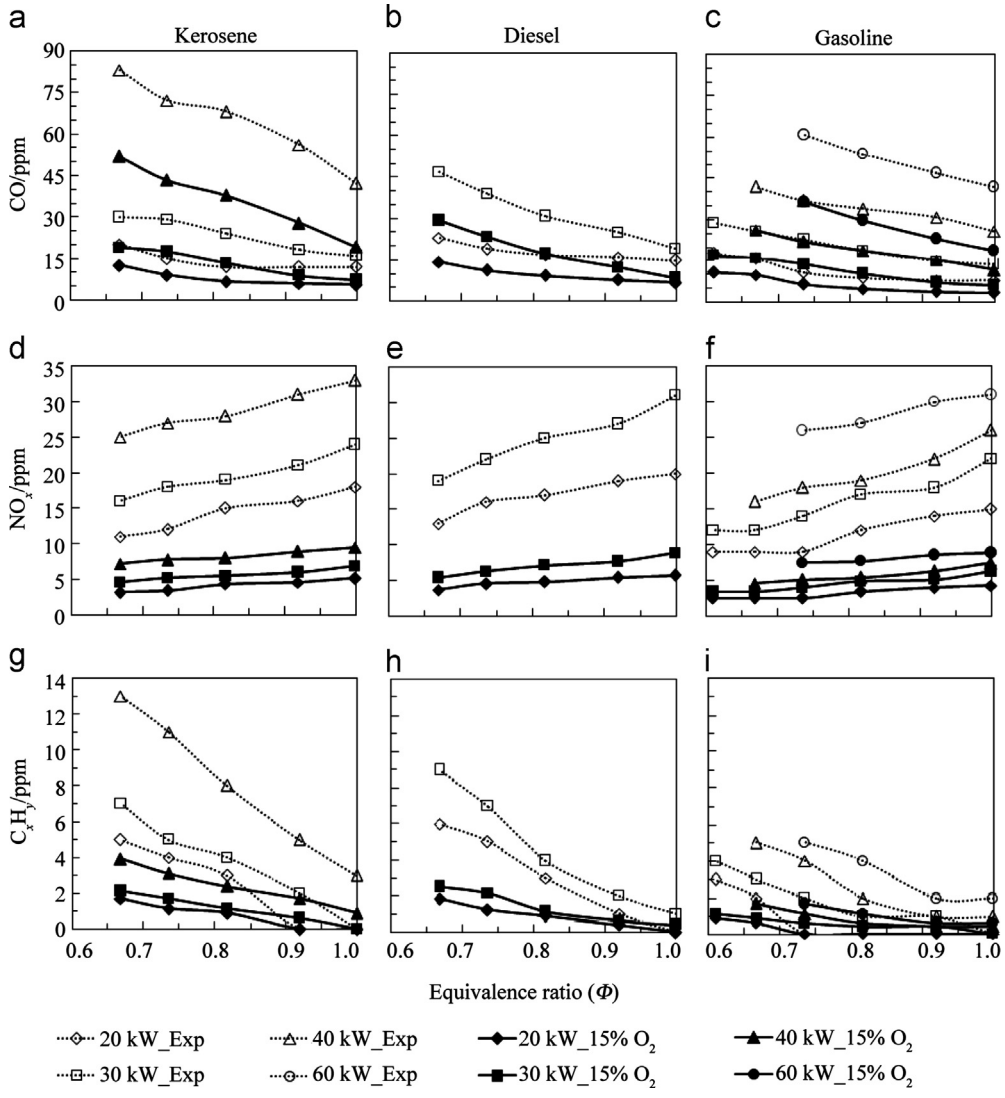


**Figure 6** Pollutant emissions variation with equivalence ratio for different thermal inputs and three different fuels of kerosene, diesel and gasoline. (a–c) CO, (d–f) $NO_x$ and (g-i) $C_xH_y$ emissions.

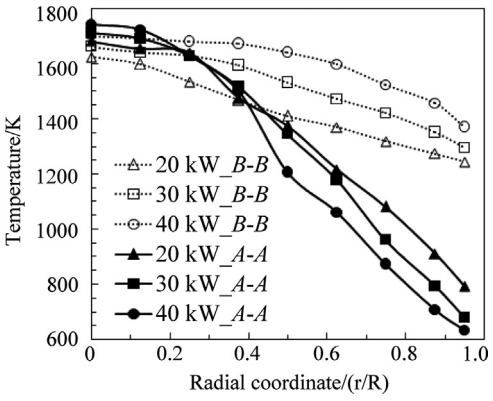


**Figure 7** Variation of temperature distribution in radial direction for D30 combustors in primary and secondary chambers at different thermal inputs.

combustion sustained till the $\Phi = 0.66$. The pollutant emissions of CO, $NO_x$ and $C_xH_y$ for different thermal inputs, equivalence ratios and fuel conditions are presented in Figure 6 (open symbols). Experimentally measured emissions are corrected to 15% $O_2$ levels and plotted in Figure 6 (solid symbols). For 20 kW thermal input and at $\Phi = 0.8$, CO emissions for kerosene, diesel and gasoline are 6, 9 and 5 ppm respectively. $NO_x$ emissions are 4, 5 and 3 ppm respectively. For case of 60 kW thermal input, flameless combustion stabilized with gasoline fuel only and some unburned fuel is accumulated for case of kerosene and diesel fuels. For 60 kW thermal input and at $\Phi = 0.81$ the CO, $NO_x$ emissions (15% $O_2$) with gasoline fuel are 23 and 8 ppm respectively.

## 5.2. Temperature distribution

The radial temperature variation in the primary and secondary chamber is measured at *A-A* and *B-B* planes (Figure 5). The temperature distribution in primary and secondary chambers (*A-A* and *B-B*) at $\Phi = 0.92$ for different thermal inputs is shown in Figure 7. Since fresh oxidizer enters through tangential inlets and creates a very strong swirl flow, the temperature in the near wall region is relatively lower in the primary chamber. Due to strong swirl flow in the near wall region, temperature gradient is relatively large in primary chamber. The temperature increases towards the center of the combustor and reaches a maximum value. At section *B-B*, a slightly different trend is observed. The temperature in the near wall region is in the range of 1000–1300 K and increases to 1650 K at the center. In the secondary chamber, the temperature at all radial locations increases with thermal input. However, in the primary chamber, the temperature at all radial locations has been observed to reduce with an increase in the thermal input. This is perhaps due to the reason that inlet mass flow rate of air increases with thermal input. Due to this, the residence time decreases for higher mass flow rates and unburned air fuel mixture is burned in the secondary chamber. It is shown in Figure 7 that at a radial location of 0.5 in the secondary chamber, the temperature for 20, 30 and 40 kW is 1410, 1532 and 1641 K respectively. At the same location of the primary chamber, the temperatures for 20, 30 and 40 kW are 1376, 1321 and 1207 K respectively. Temperature gradient in the primary chamber is relatively much higher and increases with an increase in thermal heat input. However, the temperature gradient in the radial direction decreases in the secondary chamber.

The variation of the temperature with global equivalence ratio at a location *B-B* in the D30 combustor for 20 kW thermal inputs and kerosene fuel is shown in Figure 8. The difference between the temperature at center and near-wall location decreases with an increase in the mixture equivalence ratio. This can be attributed to the increased supply of the air for lean mixtures. It can be observed from Figure 8 that for an equivalence ratio of 0.92 and 0.66, the difference in the near wall and center temperature is 382 K and 573 K respectively. The temperature distribution in central zone becomes more flat with an increase in the equivalence ratio.

## 5.3. Acoustics emissions

The variation of acoustic emissions during the operation of the combustors is shown in Figure 9. Acoustic emissions are measured on D30 combustor with kerosene fuel at an equivalence ratio of 0.98. Measurements are carried out at different instances of base level (non-reacting flow), transition and flameless mode with a sound level meter. For ambient conditions, a base level of 84 dB is measured at combustor outlet for D30 combustor. For D30 case, once the combustor is ignited, the conventional flame started converting to flameless mode through transition mode and the level of acoustic emissions reaches 102 dB. As the operating mode completely shifted to flameless mode, a decrease in the acoustic emissions to 94 dB is observed. Similar reduction in the acoustic emissions has been reported by Kumar et al. [2] on a semi-industrial 150 kW combustor. Therefore, the reduction in the acoustic

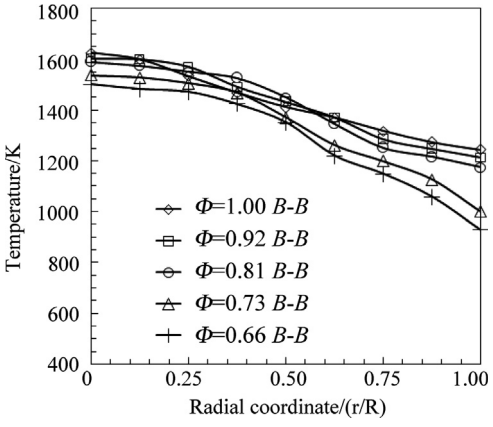


**Figure 8** Temperature variations with mixture ratio at *B-B* in D30 combustor for 20 kW thermal input (kerosene fuel).

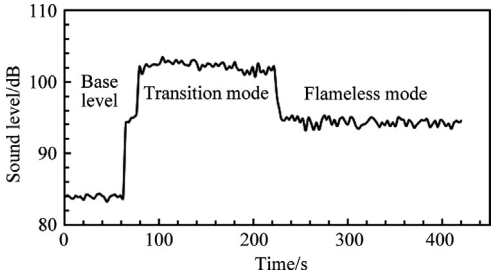


**Figure 9** Variation of acoustics emissions for D30 combustor at different modes of combustion [16].

emissions can be attributed to the change in the operation of the combustor in flameless combustion mode.

## 6. Conclusions

This paper presents the experimental and numerical results for a two stage combustor capable of achieving flameless combustion for different thermal heat inputs of 20, 30, 40 and 60 kW and heat release density of 5–15 MW/m$^3$. Combustion characteristics and pollutants emissions are measured for three different fuels of kerosene, diesel and gasoline. The study is an initial attempt towards the development of flameless combustion system with liquid fuel for various industrial and gas turbine applications. Aerothermochemical computations helped in the design of its features such as flameless combustion with reactants at ambient conditions, high heat release rates and very low CO, $NO_x$ and $C_xH_y$ emissions. The tangential air injection helps in achieving better recirculation with mixing and higher residence times. The computational results show that the decrease in the port diameter of the primary chamber increases the reactants dilution ratio ($R_{dil}$). The maximum reactants dilution ratio of 2.19 was observed for D30 combustor. A maximum dilution ratio of 2.0 and 1.9 was observed for D45 and D60 cases respectively. The D30 combustor is considered as an optimal combustor to achieve flameless combustion mode. The variation of reactants dilution ratio with thermal input and equivalence ratio is studied on D30 combustor. Reactants dilution ratio, $R_{dil}$ and length of high recirculation zone decreases with an increase in the thermal input. The reactant dilution ratio increased for leaner mixtures at a given thermal input condition. Detailed experimental investigations on D30 combustor show that very low levels of emissions are formed during the flameless combustion mode. For fuel with lower droplet diameter and lower boiling temperature case (gasoline), combustion sustained for very lean mixtures and higher thermal inputs. It is observed that CO emissions increase for leaner mixtures and $NO_x$ emissions decrease. The acoustic emission measurements show that these emissions were significantly reduced when the combustor operation shifted to flameless combustion mode from conventional combustion mode.

## Acknowledgements

The authors would like to acknowledge the funding received for this work from Aeronautics Research & Development Board (ARDB), Bangalore, India.

## References

[1] J.A. Wunning, J.G. Wunning, Flameless oxidation to reduce thermal NO-formation, Progress in Energy and Combustion Science 23 (1) (1997) 81–94.
[2] S. Kumar, P.J. Paul, H.S. Mukunda, Studies on a new high-intensity low-emission burner, Proceedings of the Combustion Institute 29 (1) (2002) 1131–1137.
[3] S. Kumar, P.J. Paul, H.S. Mukunda, Investigations of the scaling criteria for a mild combustion burner, Proceedings of the Combustion Institute 30 (2) (2005) 2613-2621.
[4] Y. Levy, V. Sherbaum, P. Arfi, Basic thermodynamics of FLOXCOM, the low-$NO_x$ gas turbines adiabatic combustor, Applied Thermal Engineering 24 (11-12) (2004) 1593–1605.
[5] T. Plessing, N. Peters, J.G. Wunning, Laseroptical investigation of highly preheated combustion with strong exhaust gas recirculation, Symposium (International) on Combustion 27 (2) (1998) 3197–3204.
[6] G.G. Szego, B.B. Dally, G.J. Nathan, Operational characteristics of a parallel jet MILD combustion burner system, Combustion and Flame 156 (2) (2009) 429–438.
[7] A. Cavaliere, M. de Joannon, Mild combustion, Progress in Energy and Combustion Science 30 (4) (2004) 329–366.
[8] M. Derudi, A. Villani, R. Rota, Sustainability of mild combustion of hydrogen-containing hybrid fuels, Proceedings of the Combustion Institute 31 (2) (2007) 3393–3400.
[9] J. Mi, P. Li, B.B. Dally, R.A. Craig, Importance of initial momentum rate and air-fuel premixing on moderate or intense low oxygen dilution (MILD) combustion in a recuperative furnace, Energy Fuels 23 (11) (2009) 5349–5356.
[10] G.G. Szego, B.B. Dally, G.J. Nathan, Scaling of $NO_x$ emissions from a laboratory-scale mild combustion furnace, Combustion and Flame 154 (1–2) (2008) 281–295.
[11] S. Kumar, P.J. Paul, H.S. Mukunda, Prediction of flame liftoff height of diffusion/partially premixed jet flames and modeling of mild combustion burners, Combustion Science and Technolgy 179 (10) (2007) 2219–2253.
[12] P. Li, J. Mi, B.B. Dally, R.A. Craig, F. Wang, Premixed moderate or intense low-oxygen dilution (MILD) combustion from a single jet burner in a laboratory-scale furnace, Energy Fuels 25 (7) (2011) 2782–2793.
[13] C. Galletti, A. Parente, L. Tognotti, Numerical and experimental investigation of a mild combustion burner, Combustion and Flame 151 (4) (2007) 649–664.
[14] R. Weber, J.P. Smart, W. vd Kamp, On the (MILD) combustion of gaseous, liquid, and solid fuels in high temperature preheated air, Proceedings of the Combustion Institute 30 (2) (2005) 2623–2629.
[15] M. Derudi, R. Rota, Experimental study of the mild combustion of liquid hydrocarbons, Proceedings of the Combustion Institute 33 (2) (2011) 3325–3332.
[16] V.M. Reddy, D. Sawant, D. Trivedi, S. Kumar, Studies on a liquid fuel based two stage flameless combustor, Proceedings of the Combustion Institute 34 (2) (2013) 3319–3326.

[17] V.M. Reddy, D. Trivedi, S. Kumar, Experimental investigations on lifted spray flames for a range of coflow conditions, Combustion Science and Technology 184 (1) (2012) 44–63.
[18] A.H. Lefebvre, Atomization and Sprays, Hemisphere, Washington DC, 1989.
[19] R. Hadef, B. Lenze, Measurements of droplets characteristics in a swirl-stabilized spray flame, Experimental Thermal and Fluid Science 30 (2) (2005) 117–130.
[20] H.Y. Kim, S.W. Baek, Investigation of $NO_x$ reduction in fuel-lean reburning system with propane, Energy Fuels 25 (3) (2011) 905–915.
[21] R.A. Yetter, I. Glassman, H.C. Gabler, Asymmetric whirl combustion: A new low $NO_x$ approach, Proceedings of the Combustion Institute 28 (1) (2000) 1265–1272.
[22] A.E.E. Khalil, A.K. Gupta, Swirling distributed combustion for clean energy conversion in gas turbine applications, Applied Energy 88 (11) (2011) 3685–3693.
[23] H.Y. Kim, S.W. Baek, Experimental study of fuel-lean reburn system for $NO_x$ reduction and CO emission in oxygen enhanced combustion, International Journal of Energy Research 35 (8) (2011) 710–720.